Carlos Garcia-Mateo, Francisca Garcia Caballero .

MATERALIA Research Group. Department of Physical Metallurgy, Centro Nacional de Investigaciones Metalúrgicas (CENIM-CSIC), Madrid, Spain.

Design of carbide-free low-temperature ultra high strength bainitic steels

There are severe limitations to attaining submicrostructured steels by means of continuous cooling, the achievement of fine grain sizes is limited by the need to dissipate enthalpy during rapid transformation, so that the actual grain size obtained is more than an order of magnitude greater than can be obtained theoretically. Bainitic microstructures obtained by isothermal heat treatment at low temperatures, can overcome the recalescence limitations and at the same time provide a very fine microstructure (nanostructure) that leads to extraordinary mechanical properties. Steel grades for this purpose have been designed by means of phase transformation theory alone and their mechanical properties tested. The results obtained reveal that the microstructure is indeed extremely fine and exhibits high levels of strength accompanied by reasonable ductility and toughness, mainly due to the fine scale of the bainitic ferrite plates achieved. The influence that retained austenite has on the mechanical properties through the TRIP effect is also discussed.

Keywords: Bainite; Phase transformation theory; Mechanical properties; TRIP

1. Introduction

From the point of view of strength and toughness in steels, it is accepted that the most common way to improve both at the same time is by refining the microstructure. Traditionally this has been achieved by applying deformation and/or rapid cooling to favour finer transformation products. It is possible to demonstrate that in the latter case, recalescence during transformation limits the final size of the microstructure.

Equation (1) [1] gives the smallest proeutectoid ferrite size that may be obtained by transformation from austenite, as a function of the free energy change per unit of volume when austenite transforms to ferrite $\Delta G_V^{\gamma\alpha}$, and the prior austenite grain size $\overline{L}_\gamma$ (mean lineal intercept)

$$\overline{L}_\alpha^{\min} = \frac{2\sigma_\alpha}{\left|\Delta G_V^{\gamma\alpha}\right| + 2\sigma_\gamma / \overline{L}_\gamma} \qquad (1)$$

where σ_γ and σ_α represent the free energy per unit area of austenite and ferrite respectively.

As expected, reduction of the austenite grain size should always lead to a corresponding reduction in the ferrite grain size. However, the magnitude of this reduction also depends on $\left|\Delta G_V^{\gamma\alpha}\right|$, i.e. on the undercooling at which the $\gamma \rightarrow \alpha$ transformation occurs. Thus, reductions in grain size in the submicrometre range require significant values of $\Delta G_V^{\gamma\alpha}$, meaning that the transformations would have to be suppressed to large undercoolings to achieve fine grain size. Yokota et al. [1] proved that experimental ferrite grain sizes obtained by transformation during continuous cooling are poorly described by Eq. (1), the reason is that during transformation the enthalpy change (ΔH) leads to recalescence. Therefore calculations should be done using as transformation temperatures $Ar_3+\Delta T$, where Ar_3 is the $\gamma \rightarrow \alpha$ transformation temperature, $\Delta T \cong \Delta H/C_\gamma$, is the increase in temperature due to recalescence, $C\gamma$ stands for the

austenite heat capacity. By doing so, it is shown that the recalescence-corrected calculations show better agreement with the experimental data, indicating that at large undercoolings, the achievement of fine grain size is limited by the need to dissipate enthalpy during rapid transformation; the actual grain size obtained is more than an order of magnitude greater than that expected theoretically by means of Eq. (1). Therefore, it is necessary to design some steel grades that adapt to an industrial process which enables isothermal transformation at large undercoolings.

As a natural consequence of their formation mechanism, bainitic microstructures appear as the most reasonable solution, the following paragraphs and sections will try to justify this assertion.

Bainite formation is understood as a $\gamma \rightarrow \alpha$ transformation governed by a paraequilibrium nucleation (only C diffuses) and subsequent displacive growth (no change in chemical composition) [2]. Bainite is expected to occur below the T_o' (*) temperature when:

$$\Delta G^{\gamma \rightarrow \alpha} < -G_{SB} \text{ and } \Delta G_m < G_N \qquad (2)$$

where $G_{SB} \cong 400$ J mol^{-1} is the stored energy of bainite and $\Delta G^{\gamma \rightarrow \alpha}$ is the free energy change of the transformation of γ without any change in chemical composition [2]. The first condition refers to the limits of growth. The second to the nucleation conditions, thus ΔG_m is the maximum free energy change accompanying the nucleation under paraequilibrium conditions. G_N is the universal nucleation function [3], and defines the minimum free energy change necessary in any steel, in order to nucleate bainite. The temperature at which both conditions are fulfilled is known as the bainite start temperature, B_S.

(*)The T_o' [2] temperature is that below which it is possible for austenite to transform to ferrite of the same chemical composition after allowing for the strain energy due to the displacements associated with the transformation.

Subsequent to the formation of a bainitic ferrite plate, the carbon trapped within the ferrite escapes to the parent austenite, at some point of the transformation this carbon enrichment will reach the critical value given by T_o' curve, and then displacive transformation to ferrite becomes impossible. Due to its negative slope, the lower the transformation temperature is the further the transformation can proceed, i.e. higher fraction of bainitic ferrite.

Bainite consists of aggregates of plates of bainitic ferrite separated by regions of residual phases consisting of untransformed austenite (γ) and/or phases such as martensite (γ′) or cementite (θ), which form subsequent to the growth of bainitic ferrite. Aggregates of bainitic ferrite plates, sharing common crystallographic orientation constitute the so called sheaves of bainite. When untransformed austenite is the residual phase, it can be found with two types of morphologies, as blocks between the sheaves of bainite and as thin films between bainitic ferrite plates.

In terms of ferrite plate thickness, it is well established [4] that it depends primarily on the parent austenite strength at the transformation temperature and on the chemical free energy change accompanying transformation. By lowering the transformation temperature, both magnitudes increase i.e. stronger austenite and more driving force, therefore there is larger resistance to interface motion and an increased nucleation rate, leading to smaller plate thickness.

For all the previous reasons, a new variant of high carbon carbide-free bainitic steels characterised by their low transformation temperatures, and as a consequence, by a very fine microstructure with plate morphology, are generating great interest (see e.g. 5–7). The combination of extremely high strength levels, accompanied by reasonable toughness and ductility, obtained by very simple isothermal heat treatment, are the consequences of a proper

alloy design, based on the understanding of the mechanisms and thermodynamic theory controlling this transformation [2, 8, 9]. It is the aim of this work, to present the theoretical approach used to design steels where such microstructures are obtained, as well as their mechanical properties and the relation found with the some relevant microstructural features.

2. Theoretical and experimental procedure

2.1. Theoretical approach for bainitic steel design

The following section provides with a description of fundamental premises used to design bainitic steels for high strength applications.

The aim is to obtain a microstructure composed exclusively by bainitic ferrite and retained austenite, thus avoiding at any instance the presence of brittle second phases,θ and γ´, that may deteriorate toughness and ductility behaviour.

To do so it is necessary to use ~ 2 wt.% Si, which retards cementite precipitation from austenite [2]. Therefore, austenite remains enriched in carbon after bainitic ferrite formation, thereby stabilising it down to ambient temperature. The resulting microstructure consists of plates of bainitic ferrite separated by carbon enriched regions of austenite.

As was mentioned, it is necessary to find steels that enable isothermal transformation at large undercoolings in order to allow for recallescence to dissipate, thus obtaining a very fine microstructure. Reducing the transformation temperature range at which austenite transform into bainite, $M_S < T < B_S$, has already been described as a way of obtaining higher fractions of thinner bainitic ferrite plates [4]. That, from a strength point of view, is a great advantage as ferrite is the stronger phase in the microstructure, and retained austenite the softer.

Reduction of both temperatures, M_S and B_S, can be achieved by tailoring the chemical composition of the steel. By same means it is also possible to further increase bainitic ferrite fraction, by displacing the T_o' curve towards higher C concentrations [2].

From the kinetics point of view, the intended microstructure should be obtained in reasonable time. As bainite nucleates at austenite grain boundaries, small austenite grain sizes provide a higher density of potential nucleation sites, thus accelerating the overall transformation. There is also the possibility to improve the transformation rate by using alloying elements that increase the free energy change for transformation, $\left|\Delta G^{\gamma\rightarrow\alpha}\right|$.

Large blocks of retained austenite, trapped between sheaves of bainite, tend to transform in service to high carbon untempered martensite, the TRIP effect or transformation induced by plasticity, having an embrittling effect on the microstructure [10, 11]. By contrast, thin films of austenite trapped between ferrite plates exhibit higher resistance to transformation, this concept from now on will be referred to as mechanical stability.

Strain induced transformation, the TRIP effect, will enhance ductility if the retained austenite particles are moderately stable against straining, and the resultant strain hardenability is held in a large strain range. The M_d temperature is defined as that above which strain induced $\gamma\rightarrow\gamma'$ transformation is impossible. If $M_d >> T_{TEST}$, strain hardening is consumed at early stages of deformation, and there is no ductility enhancement. The M_d temperature depends on retained austenite chemical composition, and elements such as C, Mn, Si and Al [12, 13] have a significant effect on stabilising austenite by decreasing M_d, C having the strongest influence.

There is also a morphological factor influencing the mechanical stability of austenite. Thin films of austenite, trapped between ferrite plates, are much more stable than blocks, partly because of their higher carbon content [12], but also because of the constraint exerted by the surrounding plates of ferrite in the microstructure. Thus, thin films of austenite with few nm thickness are too stable to transform by the TRIP effect [14, 15]. Enhancement of thin film morphology as opposed to blocky is also attained by lowering the transformation temperature [11].

All the above design concepts and theoretical considerations are summarised in a new variant of steels, carbide free low-temperature bainitic steels. A final set of two grades were selected for this work, their chemical compositions are listed in Table 1.

The alloys contain high C, to ensure good strength and low transformation temperatures. Mn and Cr to provide enough hardenability, ensuring that no other transformations interfere with bainite formation. Mo addition is made to reduce impurity embrittlement and to increase hardenability. A Si content of 1.5 wt.% avoids cementite precipitation during bainite formation, and consequently austenite becomes stable at room temperature. Finally, Co and Al were added because their ability to shift the T_o' towards higher concentrations, Fig. 1a, as well as increasing the critical driving force for transformation, see Fig. 1 b, or in other words, stimulating a more profuse ferrite formation and enhancing the transformation rate respectively.

Bhadeshia´s thermodynamic theory and kinetics models [2] together with the help of MTDATA [16] were used to perform the necessary thermodynamic calculations.

Table 1. Chemical composition in wt.% and measured start temperatures for bainitic and martensitic transformations.

	C	Si	Mn	Mo	Cr	Co	Al	P	S	M_S/ºC	B_S/ºC
Alloy 1	0.80	1.59	2.01	0.24	1	1.51	---	0.002	0.002	120	360
Alloy 2	0.79	1.56	1.98	0.24	1.01	1.51	1.01	0.002	0.002	155	385

2.2. Experimental procedure

X-ray experiments were conducted using a Phillips PPW1730 diffractometer and a scanning rate (2θ) of 0.1º min^{-1} over the range 2θ = 30–110º, with unfiltered Cu K_α radiation. The system was operated at 45 kV and 45 mA. The retained austenite content was calculated using integrated intensities of the 111, 200, 220 and 311 austenite peaks and the 110, 002, 112 and 022 peaks of ferrite. Using this number of peaks avoids possible bias due to crystallographic texture [17].The austenite and ferrite carbon content, C_γ and C_α, were calculated making use of the relationship between lattice parameter and chemical composition as reported in Refs. [18 and 19]. Ferrite X-ray data was also analysed for non-uniform strains ε. Diffraction peaks are broadened by the presence of non-uniform strains that systematically shift atoms from their ideal positions, and the finite crystallite size (coherently diffracting domain). These two effects have a different dependence on the value of the Bragg angle, θ_{hkl} [20]. The non-uniform strain effect can therefore be separated, since the slope of a plot of $\beta_{hkl} \cos\{\theta_{hkl}\}$ versus 4 $\sin\{\theta_{hkl}\}$ is equal to the strain ε. The parameter β is the measured peak broadening; it is defined as the width of a rectangle with the same area and height as the diffraction peak. In general, ε is proportional to the square root of the dislocation density [21].

The bulk material M_S temperature was determined using an Adamel Lhomargy DT1000 high-resolution dilatometer. Cylindrical specimens, 12 mm length and 2 mm diameter, were heated to 900º C at 5 K s^{-1} and then forced to cool using helium at either 100 or 200 K s^{-1}. There was no perceptible difference between the M_S temperature measures at these two cooling rates. Retained austenite M_S and M_d temperatures were calculated by means of the latest neural network model [22, 23] and Eq. (3) [24] respectively.

$$\ln V_\gamma^0 - \ln V_\gamma = k_1 \varepsilon \Delta G^{\alpha'\gamma} \qquad (3)$$

where V_γ^0 and V_γ represent the initial austenite fraction and the remaining fraction, after transformation induced plasticity, respectively. Therefore M_d corresponds to the temperature at which $V_\gamma^0 = V_\gamma$; k_1 is a constant, ε is the plastic strain and $\Delta G^{\alpha'\gamma}$ represents the chemical free energy change for the transformation of austenite to ferrite of the same chemical composition. The free energy change calculations were carried out using MTDATA with the NPL-plus data-base for steels [16].

Tensile specimens with a section of 5 mm diameter and a gauge length of 25 mm were tested at room temperature using an Instron-8032 fitted with a 100 kN load cell. A crosshead speed of 0.1 mm min^{-1} was used in all the experiments. Strain hardening was characterised by the incremental strain-hardening exponent defined as $n = d(\ln\sigma)/d(\ln\varepsilon_p)$, where $\sigma = k\,\varepsilon_p^n$ represents the flow curve in the region of uniform true plastic deformation and k is the strength coefficient.

Plane strain fracture toughness (K_{IC}) was obtained on compact tension specimens of B = 13 mm, W = 26 mm and a/W = 0.5 mm tested at room temperature in a servo-hydraulic machine. Where B and W stand for the test piece thickness and width respectively, and a for the

effective crack length. All mechanical experiments were assisted by electronic equipment that allowed the continuous tracking of load–displacement data during tests.

Specimens for transmission electron microscopy were prepared by slicing 100 μm discs and grinding them down to 50 μm thickness using 1200 grit silicon carbide paper. Subsequently they were electropolished at 50 V in a twin jet unit, using an electrolyte that consisted of 5 % perchloric acid, 15 % glycerol and 80 % ethanol in volume.

3. Results and discussion

3.1. Microstructural characterisation

As a consequence of proper design, based on phase transformation alone, both steels grades exhibit very low B_S and M_S temperatures, Table 1. Thus, it was possible to isothermally decompose austenite to bainite at temperatures as low as 300, 250 and 200 ºC. Prior to this, an austenitisation at 900 ºC for 30 min, followed by air cooling to the isothermal heat treatment temperature, was applied. The austenitisation conditions were selected in order to achieve a small austenite grain size, about 30 μm [25]. Regarding transformation kinetics, the time necessary to finish the transformation ranges from few hours at 300 ºC to 3 days at 200 ºC in both steels [25].

Characterisation of the microstructure thus obtained, by means of X-ray and metallographic analysis, is summarised in Table 2. It is confirmed that indeed the general microstructure consists of a mixture of only two phases, plates of bainitic ferrite, and carbon enriched retained austenite. As an example Fig. 2a and b show the typical microstructure obtained by transformation at 200 ºC for steel containing Co, and Fig. 2c at 250ºC for the Co+Al alloy. Both techniques, X-ray and detailed microscopy, failed to reveal any cementite or martensite

in the microstructure. According to the M_S calculation for retained austenite, Table 2, martensite is only expected if cooling from the transformation temperature is well below room temperature.

Table 2. Microstructural characterisation data. T stands for the isothermal transformation temperature in ºC, C_γ and C_α for the carbon concentration in austenite and bainitic ferrite respectively, in wt.%. V_γ and V_α stand for the fraction of retained austenite and bainitic ferrite respectively by means of X-ray, $V_{\gamma F}$ and $V_{\gamma B}$ are the fractions of thin films and blocks of retained austenite, respectively, according to Ref. [11]. M_S and M_d for the martensite start temperature and the temperature above which no strain induced transformation is possible, respectively. Finally, t is the ferrite plate thickness (nm) and ρ the dislocation density within bainitic ferrite plates (10^{15} m^{-2}).

	T	C_α	C_γ	V_α	V_γ	$V_{\gamma F}$	$V_{\gamma B}$	M_S	M_d	t	ρ
Alloy 1	200	0.35	1.1	0.87	0.13	0.129	0.0001	-10	391	30	6.7
	250	0.32	1.4	0.79	0.21	0.12	0.09	-35	301	49	4.8
	300	0.26	1.49	0.75	0.25	0.11	0.14	-40	271	64	3.21
Alloy 2	200	0.35	1.47	0.83	0.17	0.123	0.04	16	321	45	5.9
	250	0.34	1.7	0.79	0.21	0.12	0.09	-10	251	41	4.8
	300	0.29	1.9	0.63	0.37	0.09	0.28	-27	221	52	2.3

As was described above, the low transformation temperatures and the intrinsic characteristics of bainite transformation (paraequilibrium nucleation and diffusionless growth) confer the microstructure with very distinctive features, very fine ferrite plates that become coarser as transformation temperature increases, about 30 and 64 nm for alloy 1 and 45 and 52 nm for alloy 2 in the microstructures obtained at 200 ºC and 300 ºC respectively, Table 2.

Also very distinctive are the high dislocation density measured in ferrite, increasing as transformation temperature is reduced [26, 27], and the large amount of carbon which remains trapped inside the bainitic ferrite, up to 0.35 wt.%. This excess of carbon has been

independently verified using X-ray analysis and 3D atom-probe measurements [26, 28, 29]. And it has been proved, as originally suggested for martensite [30], that carbon is trapped at dislocations in the vicinity of the ferrite/austenite interface [31].

In Fig. 2 it is possible to distinguish between both types of retained austenite morphologies, as blocks between the sheaves of bainite, Fig. 2a, and as thin films between the bainitic ferrite plates, Fig.2b and c. It is well established [11] that bainitic microstructures formed at low temperatures contain retained austenite with mainly a thin film morphology. It is possible to estimate the fraction of thin films ($V_{\gamma F}$) and blocks ($V_{\gamma B}$) as a function of the transformation temperature [11], Table 2. Results thus obtained show that alloy 1 exhibit higher or equal fractions of $V_{\gamma F}$ when compared with alloy 2.

So far, it can be concluded that from a microstructural point of view we did achieve the design goals set at the beginning of this work. That is, a very fine (tens of nm) and mainly ferritic microstructure, with some retained austenite, mostly with thin film morphology, and free of brittle phases, cementite and martensite. This proves that the design premises used were correct.

3.2. Mechanical properties

The mechanical properties of the microstructures detailed in Table 2 were tested at room temperature, and results obtained are summarised in Table 3. Exhibiting an extraordinary combination of properties, yield strength (YS) greater than 1.2 GPa, and ultimate tensile strength (UTS) ranging from 1.7 to 2.3 GPa, the latter in the case of the 200 ºC microstructures. Those ultra high strength levels are accompanied by reasonable levels of fracture toughness (K_{IC}) and ductility, both decreasing as strength increases. The

microstructures obtained by transformation at 300 ºC exhibit total elongation of ~30% and fracture toughness of 44 MPa $m^{0.5}$ and 51 MPa $m^{0.5}$ for alloy 1 and 2 respectively, which are very high values if compared with those obtained by transformation at 200 ºC, where elongation is reduced ~20 % and toughness by almost half.

Table 3. Summary of mechanical properties characterisation data. *T* stands for the isothermal transformation temperature, and ε_T for the total elongation achieved during tensile tests.

	T/ºC	YS/ GPa	UTS/ GPa	ε_T/ %	K_{Ic}/ MPa $m^{0.5}$	YS/UTS
Alloy 1	200	1.4	2.2	4.6	27.5	0.6
	250	1.5	2.1	19.0	37.5	0.7
	300	1.2	1.8	29.0	44.0	0.7
Alloy 2	200	1.4	2.3	7.6	27.8	0.6
	250	1.4	1.9	9.4	31.7	0.7
	300	1.2	1.7	27.5	51.5	0.7

According to Ref. [2] there are different operative strengthening mechanisms that may contribute to ferrite strength, and those are: plate thickness, dislocation density and excess carbon in solid solution, Table 2. But as was stated, in this type of microstructure carbon is trapped at dislocations in the bainitic ferrite [31]. Therefore, there may be no independent contribution of carbon in solid solution, but rather, through its effect on the mobility of dislocations.

In relation to the microstructure-size contribution to strength, the well known Hall–Petch relation applies to coarse-grained microstructures, since it relies on the existence of sufficient space on a slip plane to build a pile-up of dislocations. On the other hand, martensite, bainite, acicular ferrite and Widmanstatten ferrite grow in the form of very fine plates or laths. The mean free path through these plates is only about twice the thickness of the plate; plate

thickness is typically sub-micrometre. Dislocation pile-ups cannot therefore form and the Hall–Petch relation ceases to apply. Instead, yielding involves the spread of dislocations which are present in the plate boundaries, between pinning points until the resulting loop hits the perimeter of the plate. When the energetics of this process are considered [32, 33], the grain size strengthening becomes $\Delta\sigma \cong 115(\bar{L}^{-1})$ where $\bar{L} \cong 2t$ is the mean linear intercept measured in μm, and $\Delta\sigma$ in MPa.

Finally, the contribution arising from dislocation density, introduced during displacive growth, is given by $\Delta\sigma \cong 7.3410^{-6}\rho^{0.5}$ [34], where ρ is in m^{-2}, and $\Delta\sigma$ in MPa .

Calculations have revealed that the biggest contribution to strength is due to the size of ferrite plates. Thus, in those microstructures obtained by transformation at 200 ºC, with >80 % of the finest bainitic ferrite, plate thickness contribution to strength is about 1.6 and 1.1 GPa for alloy 1 and 2 respectively. On the other hand, $\Delta\sigma$ due to dislocations is about 500 MPa for both alloys. Those contributions are weakened as ferrite plates become coarser, less dislocated and less profuse, i.e. as the transformation temperature is increased, see Table2. Thus for the 300 ºC microstructures, the plate thickness contribution is only about 700 MPa and between 200 and 300 MPa from the dislocation density.

So far, all the strength contributions analysed correspond to ferrite, which is the strongest and dominant phase. Therefore, it is difficult to asses the retained austenite contribution to strength in these steels. Qualitatively, austenite can affect strength by transforming to martensite during testing by the TRIP effect. The low yield/ultimate tensile strength ratios (YS/UTS) in Table 3**,** are due to the presence of austenite and the large dislocation density in the microstructure, introduced during displacive growth [35]. Consequently, retained austenite increases the strain hardening rate of the steel.

In a similar way, it can be considered that toughness and ductility are controlled by the volume fraction of retained austenite [36], also capable of enhancing ductility by its ability to transform to martensite by TRIP effect. In this sense, Fig. 3 shows the evolution of retained austenite fraction that transforms to martensite by the TRIP effect, following Eq. (3). It is obvious that a high M_d temperature leads to less stable austenite (fast transformation), and reduces the potential beneficial effect that strain induced transformation may have on ductility. According to Table 2 alloy 2 exhibits lower M_d temperatures than alloy 1, indicating that γ is expected to be mechanically more stable in the former than in the latter. This is partially due to its higher C concentration, and, moreover, because it contains about 1.01 wt.% Al which alloy 1 lacks [12, 13], see Table 1.

This assumption is supported by the fact that in alloy 1 a martensite X-ray peak appears in the spectra after 3 % true strain deformation, being an indication that the TRIP effect has effectively started. This is not observed under the same conditions in alloy 2, no $\gamma \rightarrow \gamma'$ transformation has taken place after 3 % true strain. It is important to note that according to the X-ray analysis on fracture surfaces of tensile specimens, no retained austenite is present in any of the cases, which means that all retained austenite did transform to martensite during tensile testing.

Thus, it is not surprising that those microstructures obtained by transformation at the highest temperature, high fractions of stable γ Table 2, exhibit the best results in terms of total elongation and fracture toughness if compared with stronger microstructures, e.g. those obtained at 200 ºC with lower V_γ values. Therefore, and according to Table 2, the retained

austenite in alloy 2 is intrinsically more stable that in alloy 1, or equivalently, lower M_d temperatures due to higher C and Al content.

There is a correlation between the shape of the incremental work hardening exponent *n* vs. true strain curve, Fig. 4, and the rate at which retained austenite transforms to martensite [13, 37–40]. It is then possible to sketch a possible explanation of the mechanisms occurring during tensile test.

Microstructures obtained at 200 ºC, with low fractions of very unstable austenite (high M_d temperatures), exhibit a high increase in *n* during the first stages of plastic deformation. This is followed by a drastic drop that ends at low levels of plastic deformation, meaning that γ transforms to γ´ rapidly at very small strains, consequently there is little benefit from strain induced transformation.

The situation changes as the fraction of more stable austenite increases in the microstructure (low M_d temperatures), Fig. 4. The microstructures obtained by transformation at 250 ^{o}C show different behaviour in the two alloys. In alloy 1, right after reaching its maximum, *n* smoothly decreases until the onset of necking, while in the case of alloy 2 after a fast reduction of *n* there is a clear tendency to decrease more slowly, up to the fulfilment of the instability criterion. That means that in alloy 1 γ transformation into γ´ starts at early stages and goes through to the onset of necking, the associated increase in strain hardening is able to arrest drop in *n* to higher deformations than in alloy 2. The latter has more stable γ and, therefore starts to transform at later stages, suggesting that part of the transformation is happening during necking, so retained austenite in alloy 2 is mechanically too stable.

High fractions of very stable austenite are present at 300 ºC microstructures for both alloys. As a result, transformation starts well after the maximum *n* and continues progressively up to necking. Alloy 2 contains ~10 % more of the more stable retained austenite than alloy 1, even though the total elongation of alloy 2 is slightly less than that of alloy 1, Table 3. This, and the fact that alloy 1 exhibits a remarkable *n* recovery in comparison with alloy 2, supports the idea that the retained austenite in this alloy is too stable.

According to the results in Table 2 $(V_{\gamma F})_{Alloy1} > (V_{\gamma F})_{Alloy2}$, retained austenite in the first alloy is more stable than in alloy 2. This situation does not match the experimental trend just described, therefore it can be concluded that morphology is not a determining factor in controlling the mechanical stability of retained austenite, while the chemical composition (through M_d temperature) is indeed determinant.

Finally, and to have a reference, in Fig. 5 tensile strength and fracture toughness of the present alloys and of other typical bainitic steels [41] as well as conventional maraging and quenched and tempered steels are compared. As is evident from the plot, the new variant of carbide-free bainitic steels is in a very advantageous position for different applications.

4. Conclusions

The challenge in submicrostructured steels is to obtain very fine grain size, high strength and toughness in bulk samples at a reasonable cost. It appears, however, that recalescence is likely to limit the size of the allotriomorphic ferrite grains that can be obtained during continuous cooling transformation. By contrast, displacive transformations lead to fine microstructures as a natural consequence of their atomic mechanisms.

Novel bainitic steels transformed at extremely low temperatures (200–300 ºC) were designed by means of phase transformation theory and then tested in order to characterise their mechanical properties. An attempt to correlate the properties with very distinctive features of their microstructures led to the conclusion that the extraordinarily slender plates of bainitic ferrite, in conjunction with high dislocation density in ferrite, constitute the main strengthening mechanism operating. On the other hand, ductility and toughness are controlled by the amount of retained austenite and its capability of enhancing total elongation by incrementing strain hardening. In this sense, the desirable situation is that of a mechanically stable austenite, but it has been shown that a too-stable austenite is no guarantee of better results. It was also demonstrated that the mechanical stability of the retained austenite present in these microstructures is mainly determined by its chemical composition, or the ability of decreasing M_d temperature, rather than its morphology.

C. Garcia-Mateo acknowledges financial support from the Spanish Ministerio de Educación y Ciencia for the financial support in the form of Ramón y Cajal temporal contract (RyC 2004). Some of this work was carried out under the auspices of an EPSRC/MOD sponsored project on bainitic steels at the University of Cambridge; we are extremely grateful for this support over a period of three years. The authors are extremely grateful to Prof. H.K.D.H. Bhadeshia for fruitful discussions.

References:

[1]. T.Yokota, C. Garcia-Mateo, H.K.D.H. Bhadeshia: Scripta Mater. 51 (2004) 767.

[2]. H.K.D.H. Bhadeshia: Bainite in Steels, 2nd Ed. Institute of Materials, London (2001).

[3]. C. Garcia-Mateo, H.K.D.H Bhadeshia: Mater. Sci. Eng. A, 378 (2004) 289.

[4]. S.B. Singh, H.K.D.H. Bhadeshia: Mater. Sci. Eng. A, 245 (1998) 72.

[5]. H.K.D.H. Bhadeshia: Mater. Sci. Forum 500-501 (2005) 63.

[6]. F.G.Caballero, H.K.D.H. Bhadeshia, K.J.A. Mawella, D.G. Jones, P. Brown: Mater. Sci. Technol. 17 (2001) 517.

[7]. F.G.Caballero, H.K.D.H. Bhadeshia, K.J.A. Mawella, D.G. Jones, P. Brown: Mater. Sci. Technol. 18 (2002) 279.

[8]. C. Garcia-Mateo, F.G. Caballero, H.K.D.H. Bhadeshia. ISIJ Int. 43 (2003) 1238.

[9]. C. Garcia-Mateo, F.G. Caballero, H.K.D.H. Bhadeshia: Rev. Metal. Madrid 41 (2005) 186.

[10]. H.K.D.K Bhadeshia: Mater. Sci. Technol. 15 (1999) 22.

[11]. H.K.D.K Bhadeshia, D.V. Edmonds: Met. Sci. 17 (1983) 411.

[12]. H.K.D.K Bhadeshia, D.V. Edmonds: Metall. Trans. A 10 (1979) 895.

[13]. P. J. Jaques, E. Girault, A. Mertens, B. Verlinden, F. Delanny: ISIJ Int. 41 (2001) 1068.

[14]. C.A.N. Lanzilloto, F.B. Pickering: Met. Sci. 16 (1982) 371.

[15]. N.K. Ballinger, T. Gladman: Met. Sci. 15 (1981) 95.

[16]. MTDATA: Phase diagram calculation software, (National Physical Laboratory, Teddington, UK, (2004).

[17]. M.J.J. Dickson: Journal of Applied Crystallography 2 (1969) 176.

[18]. D.J. Dyson, B. Holmes: J. Iron Steel Inst. 208 (1970) 469.

[19]. H.K.D.H. Bhadeshia, S.A. David, J.M. Vitek, R.W. Reed: Mater. Sci. Technol. 7 (1991) 686.

[20]. G.K. Williamson, W.H. Hall: Acta Metall. 1 (1953) 22.

[21]. G.K. Williamson, R.E. Smallman: Philos. Mag. 1 (1956) 34.

[22]. T. Sourmail, C. Garcia-Mateo: Compu. Mater. Sci. 34 (2005) 213.

[23]. http://www.thomas-sourmail.org/martensite.html

[24]. M.Y. Sherif, C. Garcia Mateo, T. Sourmail, H.K.D.H. Bhadeshia: Mater. Sci. Technol. 20 (2004) 319.

[25]. C. Garcia-Mateo, F.G. Caballero, H.K.D.H. Bhadeshia: ISIJ Int. 43 (2003) 1821.

[26]. C. Garcia-Mateo, M. Peet, F.G. Caballero, H.K.D.H. Bhadeshia: Mater. Sci. Technol. 20 (2004) 814.

[27]. M.K. Fondekar, A.M. Rao, A.K. Mallik: Metall. Trans. 1 (1970) 885.

[28]. H.K.D.H. Bhadeshia, A.R. Waugh in: (Eds.) The Metallurgical Society of the A.I.M.E., Proc. of the International Solid-Solid Phase Transformations Conference (1998) 993.

[29]. M. Peet, S.S. Babu, M.K. Miller, H.K.D.H. Bhadeshia: Scripta Mater. 50 (2004) 1277.

[30]. D. Kalish, M. Cohen: Mater. Sci. Eng. A. 6 (1970) 156.

[31]. F.G. Caballero, M.K. Miller, S.S. Babu, C. Garcia-Mateo, C. García de Andrés: The Minerals, Metals and Materials Society, Proc. of the International Solid-Solid Phase Transformations in Inorganic Materials Conference Vol. 1 (2005) 511.

[32]. G. Langford, M. Cohen: Trans. ASM. 62 (1969) 623.

[33]. G. Langford, M. Cohen: Metall. Trans. 1 (1970) 1478.

[34]. R.W.K. Honeycombe, H.K.D.H. Bhadeshia: Steels. Microstructure and Properties, Edward Arnold, London (1995).

[35]. A.P. Coldren, R.L. Cryderman, M. Semchysen: Steel Strengthening Mechanisms, Ann Arbor, MI, Climax Molybdenum, (1969) 17.

[36]. B.P.J. Sandvik, H.P. Nevalainen: Met. Technol. 15 (1981) 213.

[37]. P.J. Jaques, E. Girault, Ph. Harlet, F. Delannay: ISIJ Int. 41 (2001) 1061.

[38]. Y. Sakuma, D.K. Matlock, G. Krauss: Metall. Trans. 23A (1992) 1233.

[39]. K. Sugimoto, M. Kobayashi, S. Hashimoto: Metall. Trans. 23A (1992) 3085.

[40]. A. Itami, M. Takahashi,K. Ushioda: ISIJ Int. 35 (1995) 1121.

[41]. V.T.T. Miihkinen, D.V. Edmonds: Mater. Sci. Technol. 3 (1987) 441.

Figure captions

Figure 1. Effect of (a) Co addition on the T_o' and (b) Co and Co+Al addition on the free energy change $\Delta G^{\gamma\alpha}$.

Figure 2. (a) optical micrograph of alloy 1 microstructure after transformation has ceased at 200 ºC, (b) corresponding electron micrograph, (c) transmission electron micrograph of bainitic microstructure obtained in alloy 2 at 250 ºC.

Figure 3. Transformed fraction of austenite in alloy 2 v.s. plastic strain; calculation for the bainitic microstructures developed at isothermal temperatures of 200, 250 and 300 ºC.

Figure 4. Curves of the incremental work hardening exponent, *n*, of microstructures obtained by transformation at different temperatures. The straight line represents the instability criterion $\varepsilon_p = n$, the onset of necking.

Figure 5. Comparison of ultimate strength and fracture tougness of : conventional quenched and tempered steels (QT), maraging steels, bainitic steels [41] (solid circles) and new bainitic steels (solid squares).

Fig_1a

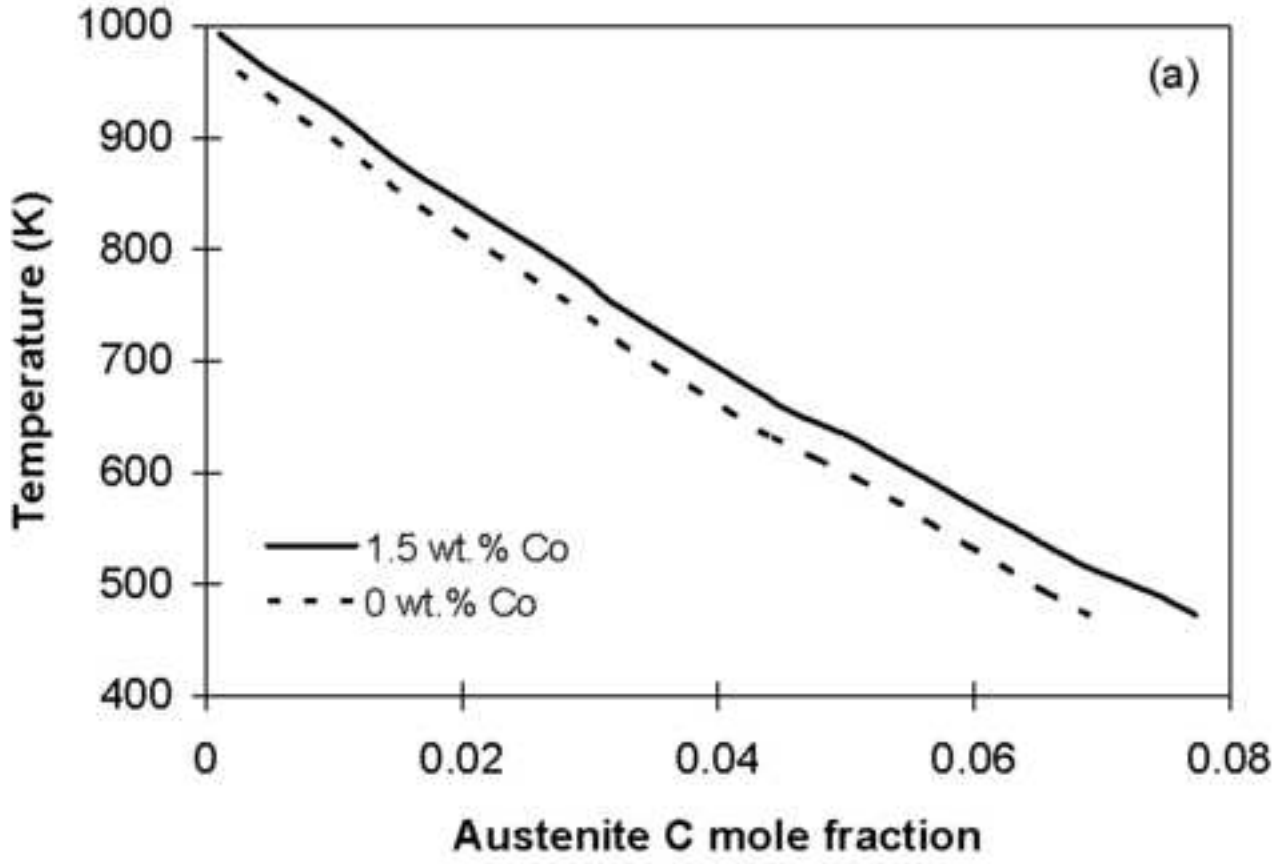
1000
900
800
700
600
500
400
Temperature (K)
(a)
1.5 wt.% Co
0 wt.% Co
0
0.02
0.04
0.06
0.08
Austenite C mole fraction

Fig.1.

Fig_1b

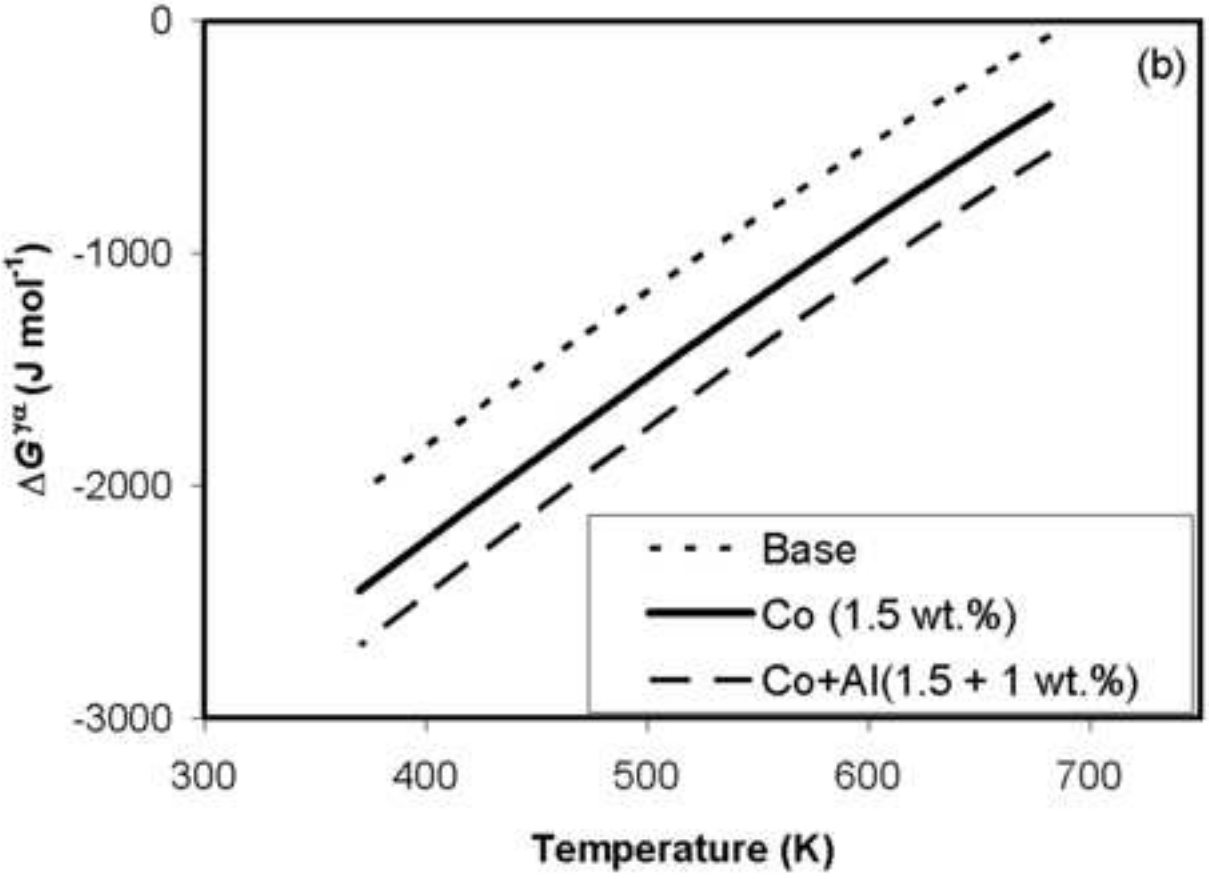
(b)
0
-1000
-2000
-3000
$\Delta G^{\gamma\alpha}$ (J mol^{-1})
300
400
500
600
700
Temperature (K)
Base
Co (1.5 wt.%)
Co+Al(1.5 + 1 wt.%)

Fig.1.

Fig_2a

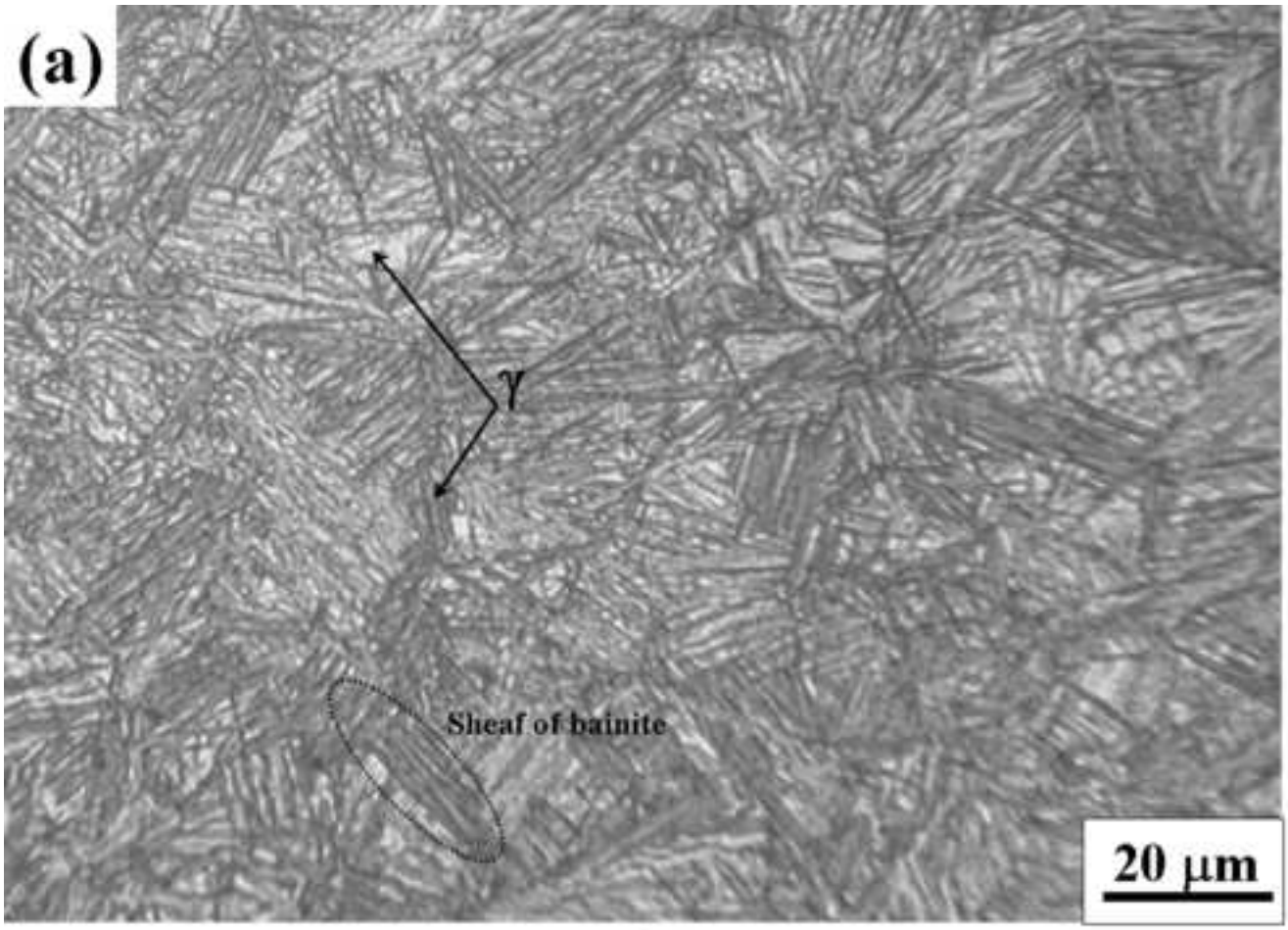

Fig.2.

Fig_2b

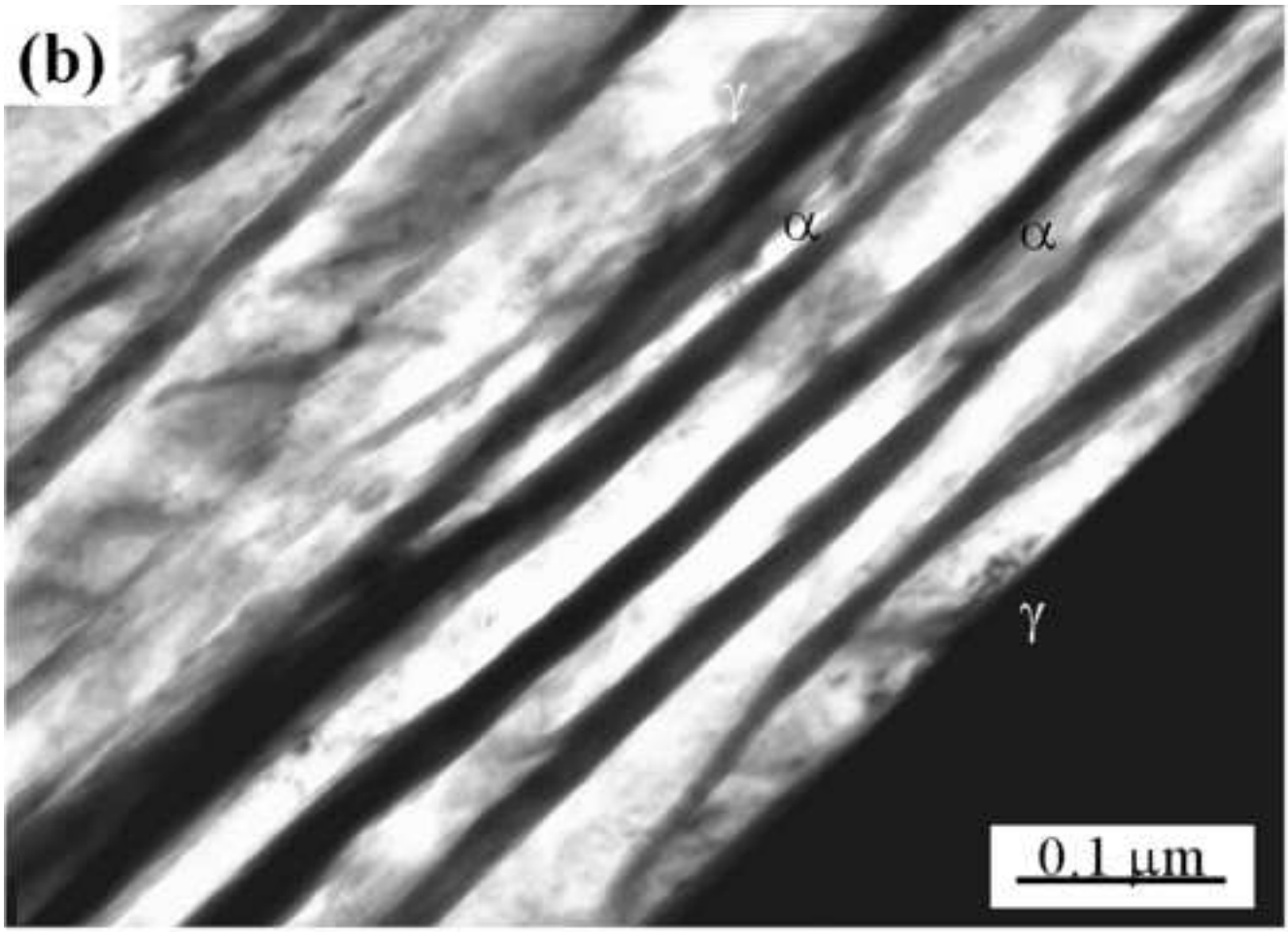

Fig.2.

Fig_2c

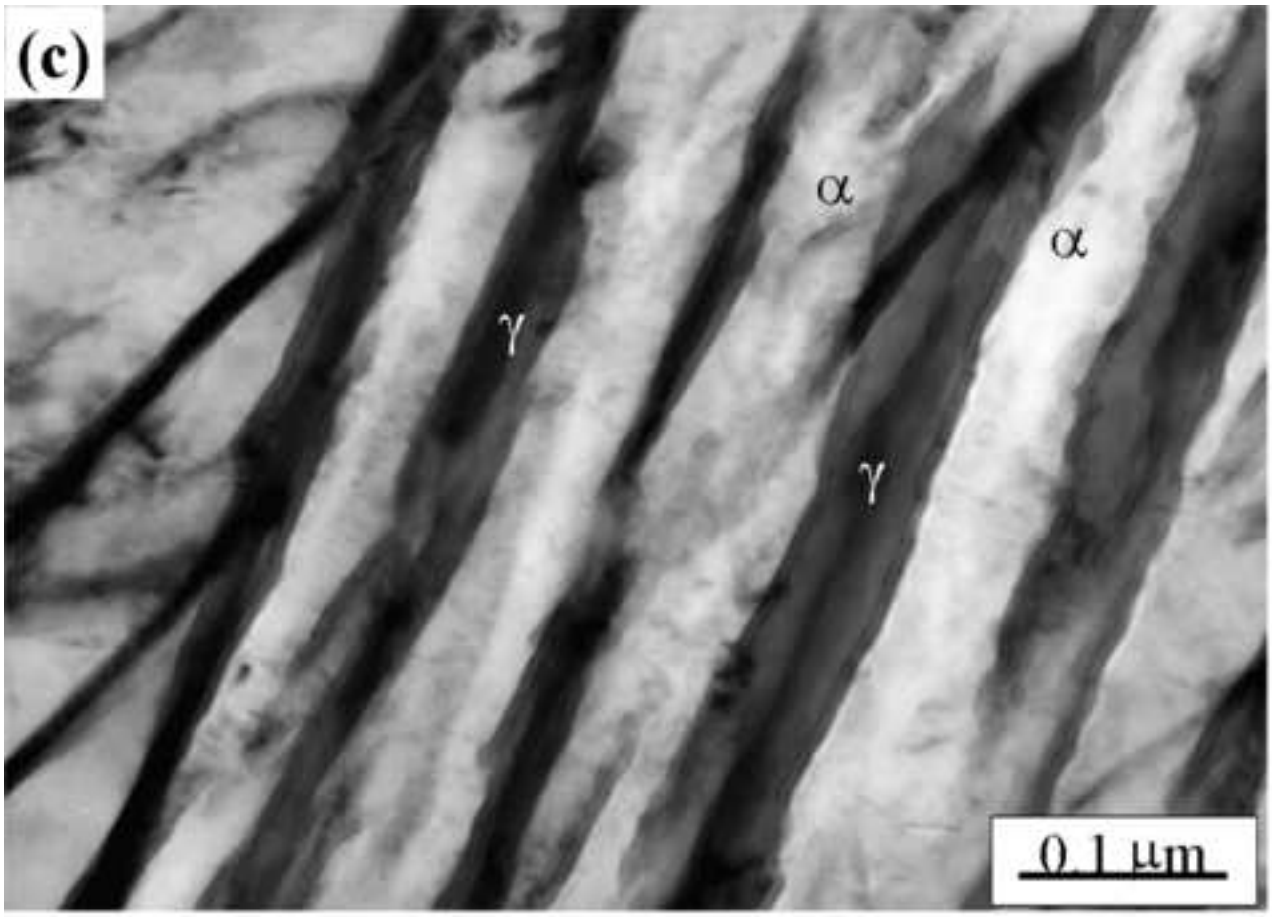

Fig.2.

Fig_3

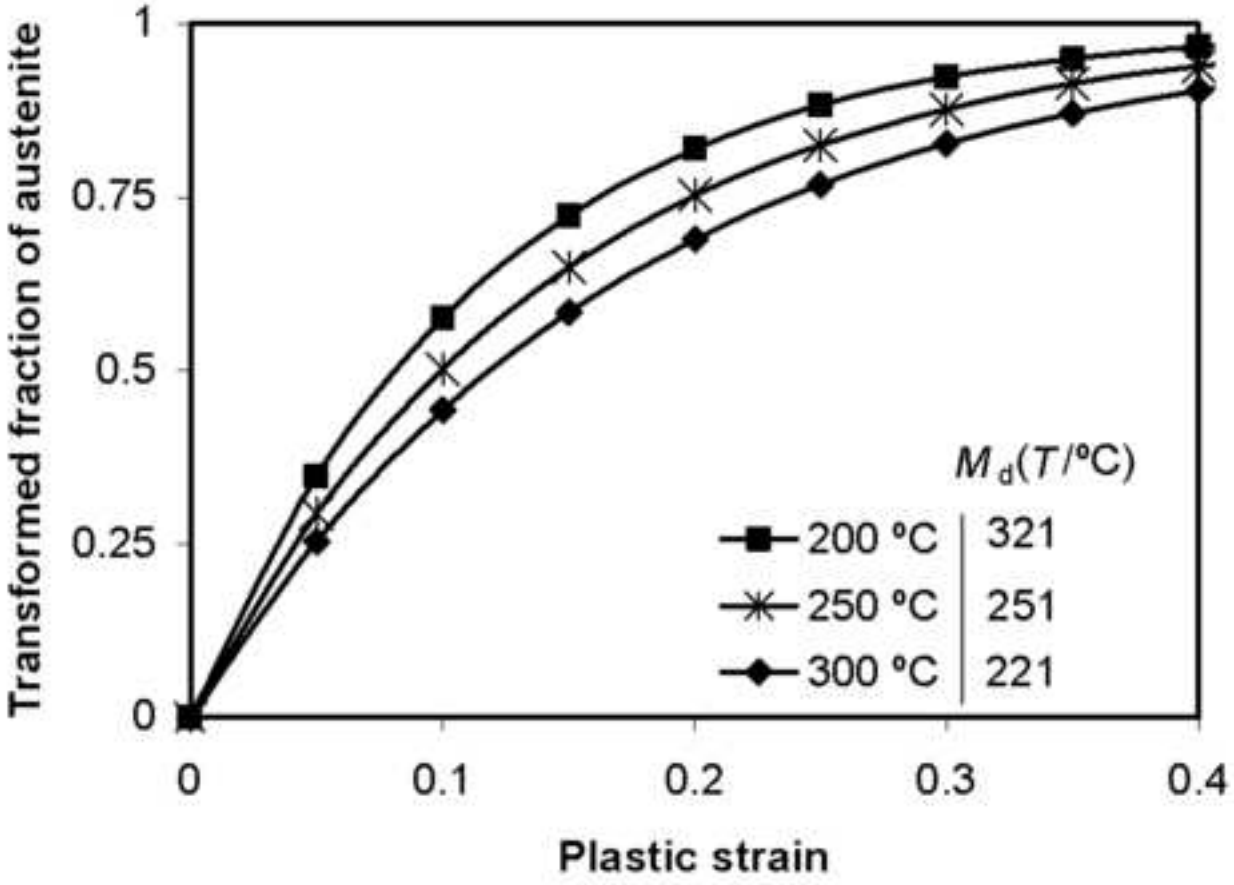
Transformed fraction of austenite
1
0.75
0.5
0.25
0
0
0.1
0.2
0.3
0.4
Plastic strain
$M_d(T/°C)$
200 °C 321
250 °C 251
300 °C 221

Fig.3.

Fig_4a

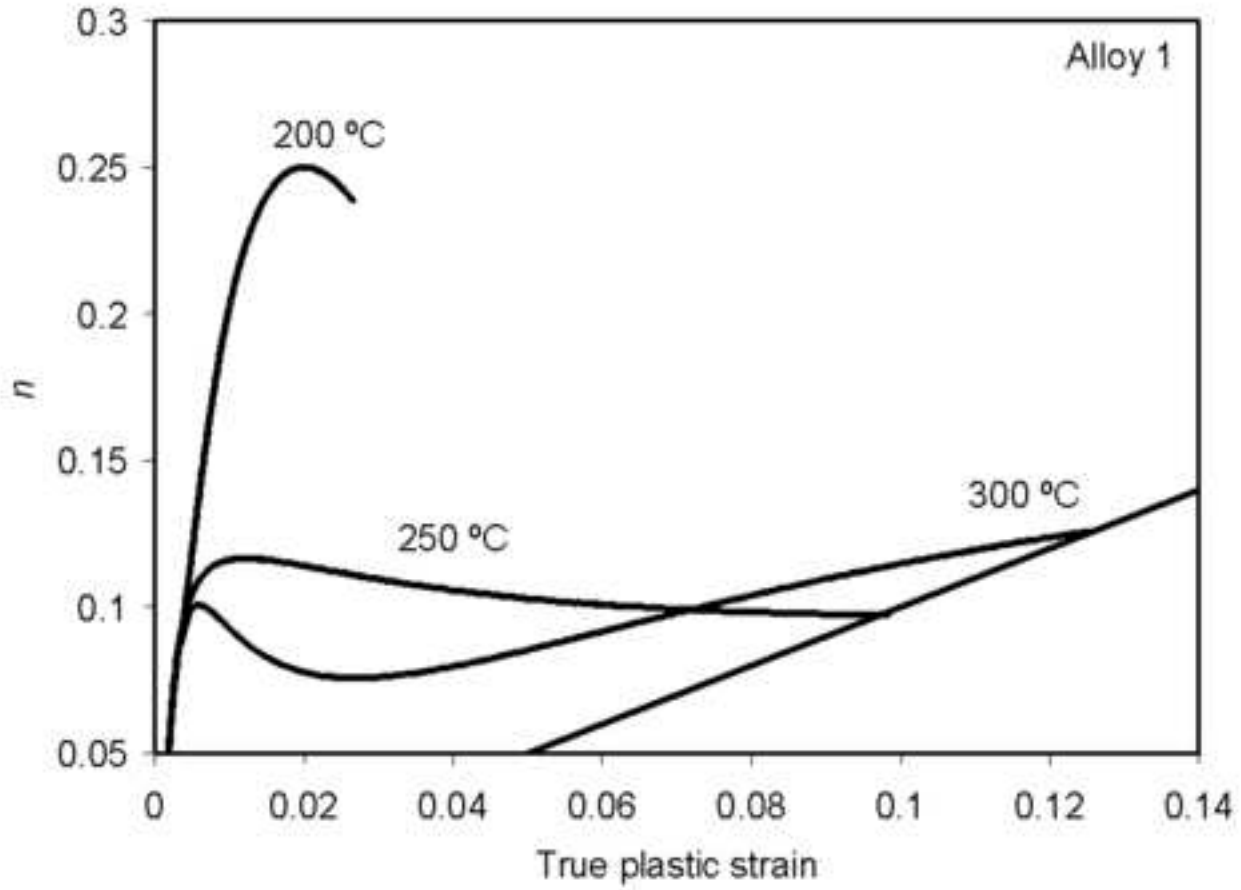
Alloy 1
200 °C
250 °C
300 °C
n
0.3
0.25
0.2
0.15
0.1
0.05
0
0.02
0.04
0.06
0.08
0.1
0.12
0.14
True plastic strain

Fig.4.

Fig_4b

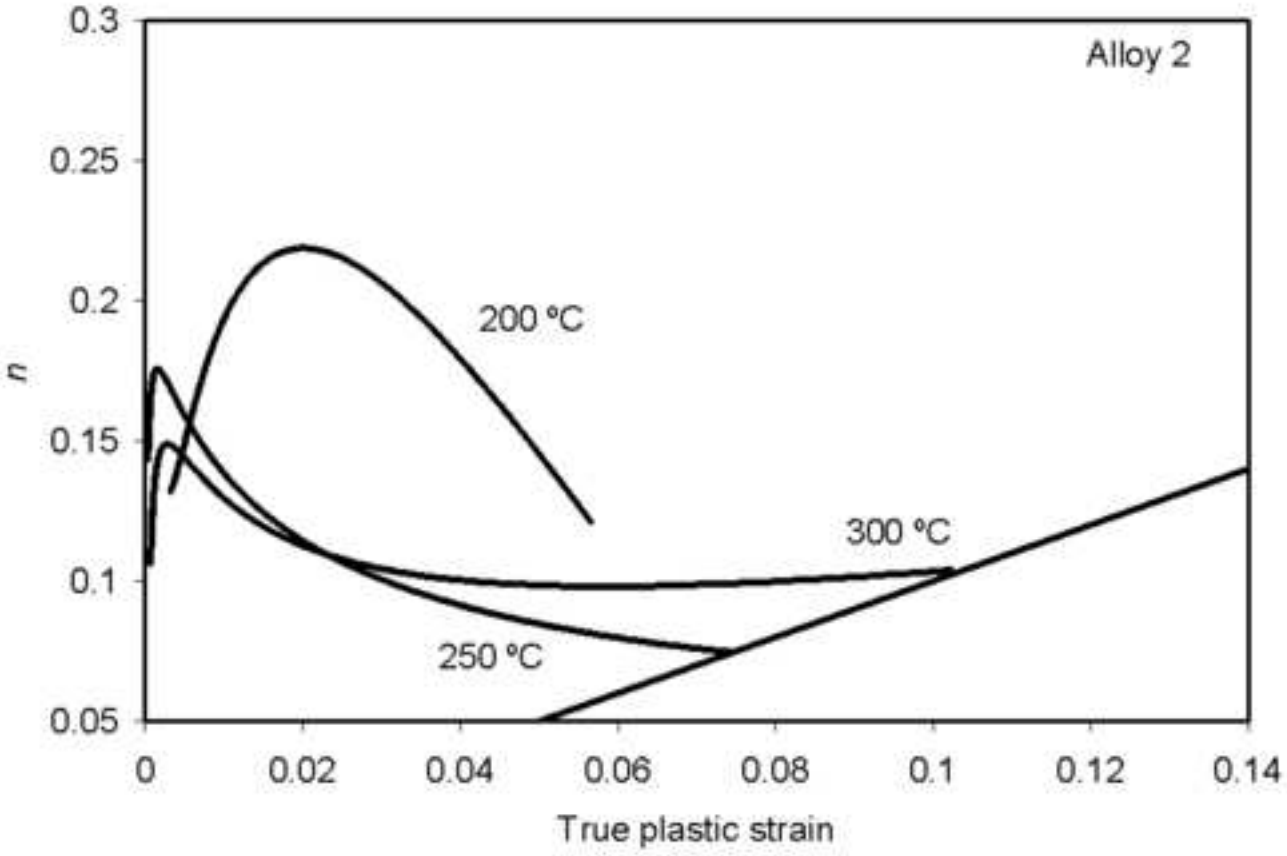
Alloy 2
200 °C
300 °C
250 °C
n
True plastic strain
0.3
0.25
0.2
0.15
0.1
0.05
0
0.02
0.04
0.06
0.08
0.1
0.12
0.14

Fig.4.

Fig_5

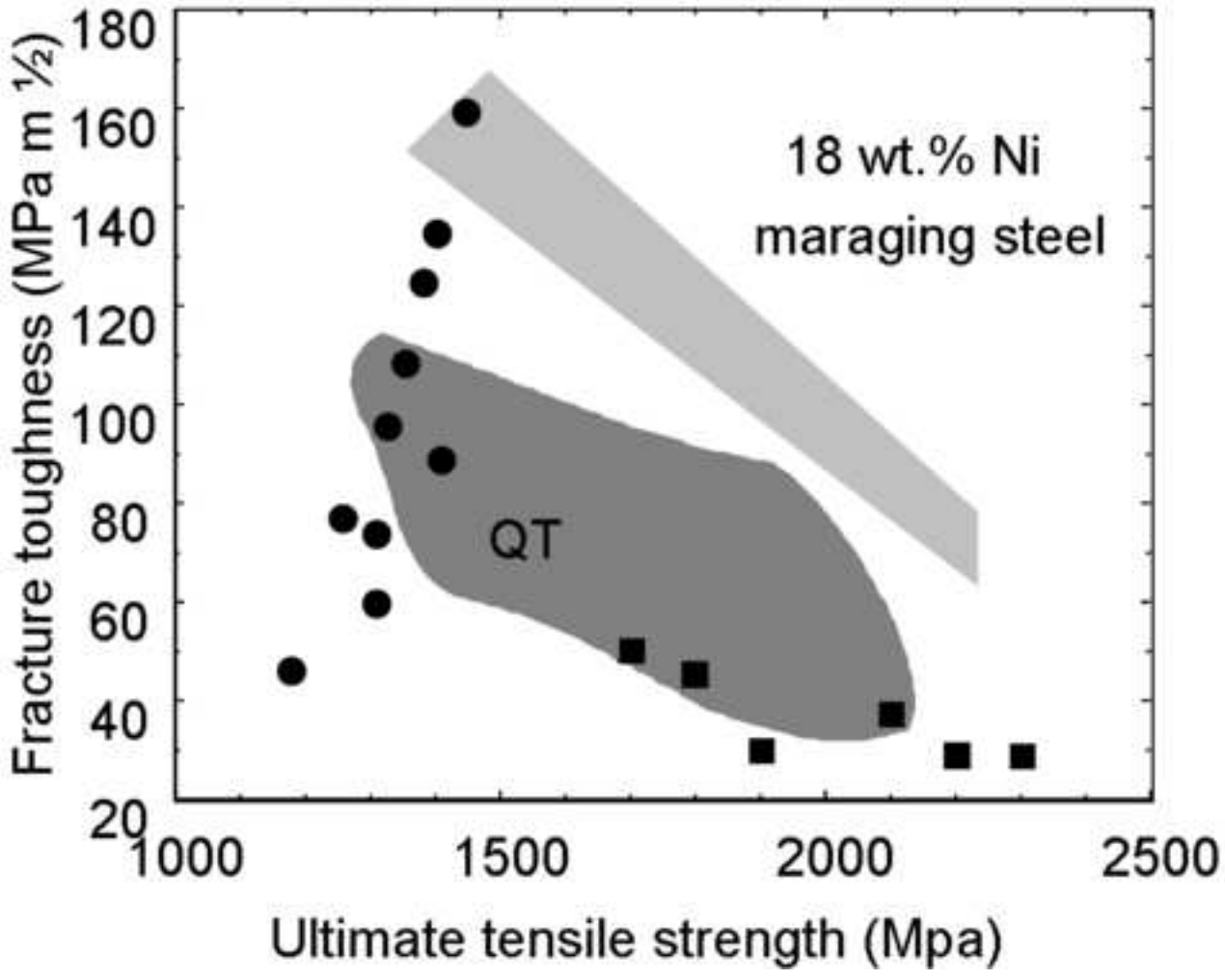
Fracture toughness (MPa m ½)
180
160
140
120
100
80
60
40
20
1000
1500
2000
2500
Ultimate tensile strength (Mpa)
18 wt.% Ni
maraging steel
QT